Computers and Geotechnics v9

September 2014

INFLUENCE OF CHOICE OF FLAC AND PLAXIS INTERFACE MODELS ON REINFORCED SOIL-STRUCTURE INTERACTIONS

Yan Yu[1], Ivan P. Damians[2] and Richard J. Bathurst[3]

[1] Postdoctoral Fellow, GeoEngineering Centre at Queen's-RMC, Department of Civil Engineering, 13 General Crerar, Sawyer Building, Royal Military College of Canada Kingston, Ontario K7K 7B4, Canada; Phone: (+1) 613 541 6000 ext. 6347, Fax: (+1) 613 541 6218, E-mail: yan.yu@ce.queensu.ca

[2] Ph.D. Candidate, Department of Geotechnical Engineering and Geo-Sciences (ETCG) and Institute for Sustainability (IS.UPC). Universitat Politècnica de Catalunya-BarcelonaTech (UPC), Spain; Phone: (+34) 93 401 1695, Fax: (+34) 93 401 7251, E-mail: ivan.puig@upc.edu

[3] Professor, GeoEngineering Centre at Queen's-RMC, Department of Civil Engineering, 13 General Crerar, Sawyer Building, Royal Military College of Canada Kingston, Ontario K7K 7B4, Canada; Phone: (+1) 613 541 6000 ext. 6479, Fax: (+1) 613 541 6218, E-mail: bathurst-r@rmc.ca (**Corresponding Author**)

ABSTRACT

The choice of structure element to simulate soil reinforcement and soil-structure interaction details for numerical modelling of mechanically stabilized earth (MSE) walls can have a significant influence on numerical outcomes. Program FLAC (finite difference method) offers three different options (beam, cable and strip element) to model the reinforcement and program PLAXIS (finite element method) has two (beam and geogrid element). Both programs use different models and properties to simulate the mechanical behaviour of the interface between dissimilar materials. The paper describes the details of the linear elastic Mohr-Coulomb interface model available in the two software packages to model material interaction and how to select model parameters to give the same numerical outcomes. The numerical results quantitatively

demonstrate the conditions that give good agreement between the two programs for the same steel strip reinforced soil-structure problem and the situations where they do not. For example, the paper demonstrates that results can be very different depending on the type of structure element used to model horizontal reinforcement layers that are discontinuous in the plane-strain direction.

Key words: Interface, Soil-structure interaction, Reinforced soil walls, Numerical modelling

1 Introduction

Mechanically stabilized earth (MSE) walls have advantages with respect to ease of construction and cost over traditional concrete gravity and cantilever retaining walls, and are now used widely around the world. However, MSE walls are complicated mechanical structures with multiple design limit states for internal, external and facing stability modes of failure. Furthermore, the interactions between the backfill soil and the facing and reinforcement components strongly affect the performance of MSE walls. The conventional approach to internal stability design of these structures is to use closed-form solutions based on classical notions of active earth pressure theory (e.g., **AASHTO 2012; BS8006 2010**). However, this approach is restricted to simple structures with simple boundary conditions, geometry and materials. For more complicated project conditions or for performance-based design, geotechnical engineers often resort to advanced numerical modelling techniques.

Two numerical methods are generally used to model MSE walls: (a) finite element method (e.g., **Cai and Bathurst 1995; Karpurapu and Bathurst 1995; Rowe and Ho 1997; Yoo et al. 2011; Damians et al. 2013, 2014a**), and (b) finite difference method (e.g., **Hatami et al. 2001; Hatami and Bathurst 2005, 2006; Huang et al. 2009, 2010; Abdelouhab et al. 2011; Damians et al. 2014b**).

The numerical modelling of MSE walls requires the use of interface boundaries to simulate the discontinuity and transfer of normal and shear stresses from the soil to the reinforcement and facing components. However, the different treatment of the internal boundaries in commercially available programs using these two different numerical techniques and choice of reinforcement structure element available in the programs may result in different numerical predictions for the nominally identical MSE wall.

The objective of this paper is to examine numerical modelling details of the load transfer within a segment comprising a precast concrete panel with steel strip soil reinforcement using the finite difference method (**FLAC; Itasca 2011**) and the finite element method (**PLAXIS 2008**). Both programs are widely used by geotechnical engineers and researchers to solve soil-structure interaction problems including MSE wall systems. A method to develop equivalent interface property values for both programs is presented. The paper also demonstrates the influence of choice of structure element on numerical outcomes using beam, cable and strip options in FLAC for the soil reinforcement and the beam and "geogrid" options in PLAXIS. Finally, the paper identifies situations where the two programs can give very different results.

2 Interface Modelling

For soil and structure zones in direct contact, two options are available to model soil-structure interaction in advanced numerical models (**Ng et al. 1997**): (a) interface elements with zero thickness to transfer shear and normal stresses from the soil to the structure; and (b) continuum elements with finite thickness. The focus of this paper is on interface elements with zero thickness that are available in FLAC and PLAXIS.

2.1 Interface Model and Properties in FLAC

The interfaces in FLAC (**Itasca 2011**) can be defined as glued, unglued, or bonded interfaces depending on the application. For the purpose of comparison with PLAXIS, unglued interfaces (where the slip or/and opening of interfaces is allowed and the plastic shear displacement occurs after the shear stress exceeds a maximum shear strength) are used in this paper. The interface properties are friction angle (φ_i), cohesion (c_i), dilation angle (ψ_i), tensile strength ($\sigma_{t,i}$), normal stiffness (k_n), and shear stiffness (k_s). The interface shear strength is governed by the Mohr-Coulomb failure criterion:

$$\tau_{s,max} = c_i + \sigma_n \tan\varphi_i \qquad [1]$$

where $\tau_{s,max}$ is the maximum shear stress at the interface under normal stress (σ_n).

The normal stress and shear stress (τ_s) are calculated based on the interface normal displacement (u_n) and shear displacement (u_s) using the following equations:

$$\sigma_{\mathrm{n}} = k_{\mathrm{n}} u_{\mathrm{n}} \qquad [2]$$

$$\tau_{\mathrm{s}} = \begin{cases} k_{\mathrm{s}} u_{\mathrm{s}} & k_{\mathrm{s}} u_{\mathrm{s}} \leq \tau_{\mathrm{s,max}} \\ \tau_{\mathrm{s,max}} & k_{\mathrm{s}} u_{\mathrm{s}} > \tau_{\mathrm{s,max}} \end{cases} \qquad [3]$$

2.2 Interface Model and Properties in PLAXIS

Interfaces using the linear elastic model with Mohr-Coulomb failure criterion in PLAXIS (**PLAXIS 2008**) are considered here for comparison with FLAC. These interfaces have properties of friction angle, cohesion, dilation angle, tensile strength, Young's modulus (E_{i}), and Poisson's ratio (v_{i}). Young's modulus and Poisson's ratio can be replaced by using oedometer modulus ($E_{\mathrm{oed,i}}$) and shear modulus (G_{i}). The values of interface properties in PLAXIS can be set using two options. The first option uses a reduction factor ($R_{\mathrm{i}} \leq 1.0$) applied to the soil material when defining soil property values (the default value is $R_{\mathrm{i}} = 1.0$, i.e. a fully-bonded interface). Hence, the interface property values are directly related to the mechanical properties of the soil forming the interface as:

$$c_{\mathrm{i}} = R_{\mathrm{i}} c_{\mathrm{soil}} \qquad [4]$$

$$\tan\varphi_{\mathrm{i}} = R_{\mathrm{i}} \tan\varphi_{\mathrm{soil}} \qquad [5]$$

$$\psi_{\mathrm{i}} = \begin{cases} 0 & R_{\mathrm{i}} < 1.0 \\ \psi_{\mathrm{soil}} & R_{\mathrm{i}} = 1.0 \end{cases} \qquad [6]$$

$$G_{\mathrm{i}} = R_i^2 G_{\mathrm{soil}} \qquad [7]$$

$$v_{\mathrm{i}} = 0.45 \qquad [8]$$

$$E_{\mathrm{i}} = 2G_{\mathrm{i}}\left(1 + v_{\mathrm{i}}\right) \qquad [9]$$

$$E_{\mathrm{oed,i}} = 2G_{\mathrm{i}} \frac{1 - v_{\mathrm{i}}}{1 - 2v_{\mathrm{i}}} \qquad [10]$$

$$\sigma_{\mathrm{t,i}} = R_{\mathrm{i}} \sigma_{\mathrm{t,soil}} \qquad [11]$$

where φ_{soil}, c_{soil}, ψ_{soil}, $\sigma_{\mathrm{t,soil}}$, and G_{soil} are the friction angle, cohesion, dilation angle, tensile strength, and shear modulus of the surrounding soil, respectively.

The second option treats the interface as a separate soil zone (with zero thickness). The interface property values are also calculated using **Equations 4-11** but the soil property values are for the interface and thus can be different from the properties of the surrounding soil. This is a more flexible approach with respect to equivalency between parameters used in FLAC and PLAXIS models, especially when the shear stiffness is available from laboratory tests or assumed from FLAC modelling as discussed below. It should be noted that Poisson's ratio is fixed with v_i = 0.45 in PLAXIS for interfaces which results in the normal stiffness $k_n = 11k_s$ for all interfaces.

2.3 Equivalent Interface Properties for FLAC and PLAXIS

The interface friction angle, cohesion, dilation angle, and tensile strength in FLAC are the same as those in PLAXIS and the same parameter values can be set directly in both programs. If the normal stiffness and shear stiffness from FLAC are known and $k_n = 11k_s$, the equivalent interface properties in PLAXIS can be found using the following equations:

$$E_i = \frac{(3k_n - 4k_s)k_s t_i}{k_n - k_s} \text{ and } v_i = 0.45 \quad [12]$$

$$E_{oed,i} = k_n t_i \quad [13]$$

$$G_i = k_s t_i \quad [14]$$

where t_i is the virtual thickness of the interface which is related to average element size and virtual thickness factor in PLAXIS (the exact value used during calculation can be found in the OUTPUT program – a post-processor in PLAXIS). For cases where $k_n \neq 11k_s$, no equivalent interface properties can be found for FLAC and PLAXIS.

If Young's modulus and fixed Poisson's ratio v_i = 0.45 (or oedometer modulus and shear modulus) at the interface with R_i = 1.0 (using the second option for setting interface property values) are provided from PLAXIS, the following equations can be used to compute the equivalent interface properties in FLAC:

$$k_n = \frac{E_i(1-v_i)}{(1+v_i)(1-2v_i)t_i} = \frac{E_{oed,i}}{t_i} \quad [15]$$

$$k_s = \frac{E_i}{2(1+v_i)t_i} = \frac{G_i}{t_i} \quad [16]$$

It should be noted that **Equations 4-11** are used in this investigation to calculate interface property values including those in **Equations 15-16** that are used in turn to compute k_n and k_s for FLAC simulations. If the soil Poisson's ratio is not 0.45 and reduction factor $R_i < 1.0$ are assumed for the interfaces, Young's modulus, Poisson's ratio, oedometer modulus and shear modulus for **Equations 15-16** are computed using **Equations 9, 8, 10** and **7**, respectively, in PLAXIS simulations.

3 Problem Definition and Parameter Values

3.1 Unit Cells

Figure 1 shows the unit cells (dimensions of 1 m×1 m) that were modeled in this paper. The unit cell approach with concrete in the top cell was found to be the simplest method to examine equivalent interface properties for the same geometry and boundary conditions using FLAC and PLAXIS programs. Two cells were considered for each test. The material in the bottom cell was soil and the top cell was concrete. The property values for the concrete and the interface are given in **Table 1**. The soil property values are unrestricted because of the fixed boundary conditions. The surcharge load was applied to the top surface of the upper cell. All boundaries of the lower cell (including the top boundary of the lower cell) were fixed in both the *x*- and *y*-direction. All boundaries of the upper cell were free in both the *x*- and *y*-direction. On the left side of the upper cell, prescribed displacements were applied in the *x*-direction after surcharging. The concrete was modeled as a linear elastic medium. The Mohr-Coulomb failure criterion was applied to the interface. Other details for FLAC and PLAXIS simulations are given below:

- In FLAC (**Figure 1a**), each cell was modeled by one zone. The zero-thickness interface was located between the upper and lower cells.
- In PLAXIS (**Figure 1b**), each cell was modeled using two 15-node triangle elements. One 10-node interface element with zero thickness was located between the upper and lower cells.

The interface normal stiffness and shear stiffness were first assumed in FLAC and the equivalent interface properties for PLAXIS were calculated using **Equations 12-14**. The number of zones in FLAC (and the number of elements in PLAXIS) has no effect on the numerical results because of the very high elastic modulus assigned to the concrete and the fixed boundary conditions of the soil.

3.2 Single Precast Concrete Panel Segment

To better understand the load transfer from the backfill soil to the adjacent structures, a single precast concrete panel segment was simulated as shown in **Figure 2**. The panel has a height of 1.5 m, a thickness of 0.18 m, and an out-of-plane width of 1.35 m. These dimensions fall within the range of panel dimensions reported in the literature for steel reinforced soil wall systems. However, actual dimensions are not critical to the qualitative outcomes in this investigation. The modelled backfill soil zone is 5.0 m long and 1.5 m high and is supported by a smooth rigid foundation.

Three cases were examined. For all cases, the top of the backfill soil was free in both the *x*- and *y*-direction and the bottom of backfill soil was fixed in the *y*-direction. The right side of the backfill soil was fixed in the *x*-direction. Other boundary conditions and geometric details are given below for each case:

- Case 1 (**Figure 2a**): the panel was fixed in the *x*-direction and the bottom of the panel was fixed in the *y*-direction. The purpose of Case 1 is to model the transfer of normal and shear stresses from the backfill soil to the facing panel without the reinforcement.

- Case 2 (**Figure 2b**): two 4 m long by 0.1 m wide steel reinforcement layers (the thickness of each strip is 0.0023 m) were attached to the back of each facing panel at *y* = 0.75 m. These dimensions correspond to a steel strip reinforced soil wall reported by **Chida et al. (1979)**. Today most of these steel strip reinforcement products are narrower (e.g., 50 mm; **Allen et al. 2004**). However, qualitative comparisons are unaffected by the choice of steel strip reinforcing elements in this range. The steel reinforcement is located horizontally in the backfill soil with *x* = 0 - 4.0 m and *y* = 0.75 m. No restriction was applied to panel movement in the *x*-direction other than the bottom of the facing was fixed in both *x*- and *y*-direction.
- Case 3 (**Figure 2c**): the only difference between Case 2 and Case 3 is that the steel reinforcement in Case 3 is located in the backfill soil by defining three points (point one at *x* = 0 and *y* = 0.75 m, point two at *x* = 0.05 m and *y* = 0.745 m, and point three at *x* = 4.0 m and *y* = 0.745 m).

In both FLAC and PLAXIS, the facing panel is modelled using beam elements and the Mohr-Coulomb model is applied to the backfill soil. Using element (or zone) size smaller than that used in this study for both programs was shown to have only minor effect on the numerical results reported later. The details using FLAC are provided below:

- For Cases 1, 2 and 3, a total of 20 beam elements for the facing panel and 2000 zones for the backfill soil were employed. The interface was applied between the facing beam elements and backfill soil.
- For Cases 2 and 3, three different types of structure elements were used (beam, cable and strip type) with a total of 80 elements defined using *x*- and *y*-coordinates to simulate the steel strips. It should be noted that when using beam elements in FLAC, the extension of the interface is not necessary because beam elements are defined using coordinates in this paper.
- For Case 3 with beam elements for the reinforcement, no interface was applied between *x* = 0 and 0.05 m (the interfaces are applied on both sides of beam elements between 0.05 and 4.0 m).

In PLAXIS simulations, using a beam element with near zero bending stiffness for the steel reinforcement is equivalent to the geogrid element which is used hereafter. The following are details using PLAXIS:

- For Cases 1, 2 and 3, the panel was modelled using 5-node beam elements (total of 8 elements) and the backfill soil was modelled using 15-node triangle elements (total of 202 elements). The 10-node interface elements with zero thickness were applied between facing beam elements and backfill soil elements.
- For Case 2, the steel reinforcement is modelled using 5-node geogrid elements with a total of 21 elements and the interfaces between the geogrid elements and backfill soil were extended to x = 4.25 m (the end of the reinforcement is at x = 4.0 m).
- For Case 3, one "anchor" was applied for the short connection portion of the steel reinforcement between x = 0 and 0.05 m (**Figure 2c**; note that the anchor in PLAXIS only transfers load between two points). The remainder of the steel reinforcement was modelled using 21 5-node geogrid elements (both anchor and geogrid elements have the same axial stiffness). The interfaces between the geogrid elements and backfill soil (x = 0.05 - 0.4 m) were extended to x = 0.025 and 4.25 m to avoid stress concentration near x = 0.05 and 4.0 m, respectively.

As shown in **Table 2,** all interfaces have the same interface property values equivalent to those for R_i = 0.3 applied to the backfill soil in PLAXIS. It should be noted that R_i = 0.3 is generally lower than that commonly used for retaining walls with concrete facing. However this lower reduction factor can be justified to account for the effect of light compaction equipment that is recommended immediately behind the facing in current reinforced soil wall construction practice. However, the general conclusions made in this paper remain valid when the reduction factor for the interfaces between the facing and backfill soil and between the steel reinforcement and backfill soil is set to other values (e.g., the commonly used reduction factors are in the range R_i = 0.6 - 0.9). Interface property values other than those listed in **Table 2** are examined later and numerical outcomes are investigated in the corresponding sections. The equivalent interface properties for FLAC were evaluated using **Equations 16-17**. The small strain mode was used in both programs. Uniformly distributed surcharge load was applied to the top surface of the backfill soil at three different magnitudes (q = 10, 50 and 100 kPa). The backfill soil was initially brought to equilibrium using $K_0 = 1\text{-}\sin(\varphi_{soil}) = 0.305$ for both programs. Parameter values used in both programs are shown in **Table 2**. It should be noted that, when cable and strip elements in FLAC are used to model the steel reinforcement, their property values are calculated from **Table 2** based on the definition of these properties in FLAC (**Table 3**).

In the simulations to follow the out-of-plane width of the reinforcement is 0.1 m and the total out-of-plane width modelled for the facing panel and backfill soil is 0.675 m (**Figure 2**). For the reinforcement using FLAC beam elements and PLAXIS geogrid elements, the modelled interface between the steel reinforcement and backfill soil has an out-of-plane width of 0.675 m (this is the only choice for these two element types). When using FLAC cable elements and strip elements, the out-of-plane width of the interface can be less than 0.675 m. For example, the true width of the steel strip in this paper is 0.1 m corresponding to 15% area coverage ratio. However, depending on the steel reinforcement product this coverage ratio could be as high as 50% for some steel bar mat and welded wire products (**Allen et al. 2004**). For the case of geosynthetic sheet reinforcement products the coverage ratio is 100%. It should be noted that for cable and strip elements in FLAC, the interface-related properties are part of the cable and strip element properties. In the simulations to follow the above conditions apply unless noted otherwise.

4 Results

4.1 Modelling of Interfaces using Unit Cells

Table 4 shows interface normal displacements and shear stresses under different applied surcharge loads and displacements. The results from both FLAC and PLAXIS are compared with the analytical solutions (**Equations 2** and **3**). For the applied surcharge load q = 10 kPa, the exact normal displacement at the interface (with $k_n = 1.1\times10^7$ Pa/m) using **Equation 2** is $u_n = \sigma_n/k_n = 10000/1.1/10^7 = 9.09\times10^{-2}$ m = 0.909 mm. The maximum shear stress using **Equation 1** is calculated to be $\tau_{s,max} = c_i + \sigma_n\tan\varphi_i = 1000+10000\times\tan(40°) = 9.39\times10^3$ Pa = 9.39 kPa. Thus the exact shear stress at the interface (with $k_s = 1.0\times10^6$ Pa/m) using **Equation 3** under the applied shear displacement u_s = 5 mm is $\tau_s = k_s u_s = 1.0\times10^6\times5\times10^{-3} = 5.0\times10^3$ Pa = 5.0 kPa (<

9.39 kPa; the shear stress is at the elastic state). For the applied shear displacement u_s = 10 mm, the exact shear stress is $\tau_s = \tau_{s,max}$ = 9.39 kPa (due to $k_s u_s = 1.0\times10^6\times10\times10^{-3} = 10.0\times10^3$ Pa = 10.0 kPa > 9.39 kPa; the shear stress is at the plastic state). The same procedure is used to evaluate the normal displacements and shear stresses under other applied surcharge loads and displacements. The numerical results in **Table 4** show that the calculated normal displacements and shear stresses from FLAC and PLAXIS analyses agree very well with the exact solutions.

4.2 Interface Normal and Shear Stresses between Facing and Backfill Soil for Case 1

Figure 3a shows the normal stresses acting at the interface between the facing and backfill soil for Case 1 (without steel strips) and three different surcharge pressures. For q = 10 kPa, the normal stress from PLAXIS was 0.64 kPa at the top of the interface (compared to 0.83 kPa using FLAC) and increased to 13.2 kPa at the bottom of the interface (compared to 13.0 kPa - FLAC). Increasing the surcharge to q = 50 kPa, the normal stresses at the top and bottom of the interface using PLAXIS increased to 6.31 kPa (9.01 kPa - FLAC) and 32.3 kPa (32.1 kPa - FLAC), respectively. When the surcharge was q = 100 kPa, the normal stresses from PLAXIS were 13.5 kPa at top (19.7 kPa - FLAC) and 56.1 kPa at bottom of the interface (55.9 kPa - FLAC). The normal stresses from PLAXIS and FLAC are judged to be in generally good agreement. The small visual differences in normal stresses near and at top of the interface are due to the large plastic deformations in this region that resulted in small differences in predicted normal displacements between programs.

The shear stresses on the interface between the facing and backfill soil for Case 1 are shown in **Figure 3b**. When the surcharge load was q = 10 kPa, the shear stress using PLAXIS was 0.48 kPa at top of the interface (0.50 kPa - FLAC), increasing to a maximum value of 2.60 kPa at y = 0.84 m (2.57 kPa from FLAC at y = 0.83 m), and thereafter decreasing to zero at bottom of the interface. For q = 50 kPa, the shear stress at y = 1.5 m was 2.13 kPa from PLAXIS (2.80 kPa from FLAC) and the maximum shear stress was 8.47 kPa from PLAXIS at y = 0.52 m (7.94 kPa from FLAC at y = 0.53 m). Increasing the surcharge load to q = 100 kPa increased the shear stress at y = 1.5 m to 4.21 kPa from PLAXIS (5.75 kPa from FLAC) and the maximum shear stress to 15.1 kPa at y = 0.47 m (14.0 kPa from FLAC at y = 0.53 m). The slight difference for shear stresses near and at y = 1.5 m between PLAXIS and FLAC was because the predicted normal stresses from both programs were slightly different in this area (**Figure 3a**) which resulted in different computed maximum shear stress (**Equation 1**). The difference in shear stresses using the two programs is greatest near the location of maximum shear stress, especially for q = 100 kPa. This is due to differences in predicted shear displacements when slippage (interface shear failure) occurred.

4.3 Reinforcement and Facing Panel Axial Loads for Case 2

The reinforcement axial loads for Case 2 with PLAXIS geogrid elements and FLAC beam elements are shown in **Figure 4**. Using PLAXIS, the reinforcement connection load was about 6.33 kN/m for the applied surcharge load q = 10 kPa. It increased to 21.1 and 39.8 kN/m when increasing the surcharge load to q = 50 and 100 kPa, respectively. For FLAC, the reinforcement connection loads were 6.55, 22.7, and 42.3 kN/m for surcharge loads q = 10, 50, and 100 kPa, respectively. The results for the reinforcement axial load (Case 2) from PLAXIS generally agreed well with those from FLAC. **Figure 4** also showed that the predicted reinforcement axial load decreased to near zero at the tail of the reinforcement in both PLAXIS and FLAC simulations. This must be the case at this boundary and thus serves as a check on the validity of numerical outcomes.

Figure 5 shows the facing panel axial loads for Case 2 with PLAXIS geogrid elements and FLAC beam elements. Recall that in Case 2 the reinforcement was located at y = 0.75 m (**Figure 2b**) and the mesh and reinforcement position in PLAXIS and FLAC were not updated during calculations using the small strain option. Thus the reinforcement generates only horizontal tensile load. The down-drag force (i.e., vertical load) on the facing panel from the reinforcement is zero. However, a sharp increase in facing axial load at the reinforcement elevation was observed for all three surcharge loads (**Figure 5**) using both programs. For example, using PLAXIS the facing axial load at y = 0.75 m jumped from 4.08 to 4.76 kN/m when q = 10 kPa, from 5.74 to 8.72 kN/m when q = 50 kPa, and from 7.80 to 13.6 kN/m when q = 100 kPa. These jumps in facing axial load were not from reinforcement down-drag forces, but are the result of unbalanced vertical force between the upper and lower sides of the reinforcement as shown in

Figure 6. This is the result of the two interface nodes (one above the reinforcement and the other one below the reinforcement) sharing the same physical position with the beam node at $x = 0$ and $y = 0.75$ m.

For Case 2 shown in **Figure 5**, the calculated facing axial loads from PLAXIS generally agreed well with those from FLAC. The slight difference in axial loads for the facing panel below the reinforcement layer ($y \leq 0.75$ m) was due to slightly different normal stress on the upper side of the reinforcement at $x = 0$ and $y = 0.75$ m calculated by the two programs. For example, when $q = 100$ kPa the normal stress on the upper side of the reinforcement at $x = 0$ and $y = 0.75$ m was about 380 kPa from PLAXIS and about 284 kPa from FLAC as shown in **Figure 6**. The modeling also showed that the calculated interface normal stresses on the upper and lower sides of the reinforcement using PLAXIS were in generally good agreement with those from FLAC (**Figure 6**). The difference near the tail-end of the reinforcement was because of the extended interface adopted in PLAXIS to avoid stress concentration near the tail.

4.4 Reinforcement Modelled by Structure Elements without Normal Stiffness for Case 2

The previous section used beam elements in FLAC to model the steel reinforcement. However, more often cable and strip structure elements are used in FLAC for this type of application (**Abdelouhab et al. 2011**). In this section, both cable and strip elements are assumed to have an interface on each side of the reinforcement with out-of-plane width of 0.675 m as in the previous section (the influence of true out-of-plane thickness of 0.1 m for typical steel strip reinforcement is examined later). It should be noted that the cable and strip elements in FLAC only have shear stiffness (no normal stiffness is specified) and the backfill soil can move through the plane of reinforcement without restriction when using cable and strip elements. The results using cable and strip elements were the same for all cases and conditions examined in this paper and thus for brevity the results with cable elements are not reported in this paper.

Figure 7 shows the reinforcement axial loads for Case 2 using PLAXIS geogrid elements and FLAC strip elements. The reinforcement connection loads at different surcharge loads from FLAC with strip elements were similar to those from FLAC with beam elements (**Figure 4**).

Good agreement between calculated reinforcement tensile loads using PLAXIS with geogrid elements and FLAC with strip elements can be seen in **Figure 7**.

The calculated facing panel axial loads for FLAC with strip elements are shown in **Figure 8** and compared with those from PLAXIS with beam elements. The FLAC results show the facing panel axial load increasing gradually from top to bottom of the facing with no jump. This confirms that the sudden change in the facing axial load at y = 0.75 m (**Figures 5** and **8**) was due to the unbalanced vertical force at x = 0 and y = 0.75 m between the upper and lower interfaces of the reinforcement when normal stiffness was applied (**Figure 6**).

4.5 Reinforcement and Facing Panel Axial Loads for Case 3

The previous sections have shown that the calculated facing axial loads can be different when using different structure elements in FLAC, and they are also different when using strip elements in FLAC and geogrid elements in PLAXIS with the same out-of-plane width. Hereafter, the short connection segment between the reinforcement and facing panel shown **Figure 2c** was included in numerical simulations using both programs.

Figure 9 shows the reinforcement axial loads for Case 3 with PLAXIS geogrid elements and FLAC beam elements. For the surcharge load condition q = 10 kPa, the reinforcement connection load was 6.52 kN/m and the reinforcement axial load gradually decreased to near zero at x = 4.0 m. The steel strip connection load was 22.3 and 42.2 kN/m when q = 50 and 100 kPa, respectively. The results show that the reinforcement axial loads predicted from both programs are in very good agreement using geogrid and beam elements.

For Case 3, the facing axial loads due to the interface shear stresses from backfill soil and down-drag loads from the reinforcement are shown in **Figure 10**. Recall that the steel strips were modelled using geogrid elements in PLAXIS and beam elements in FLAC. For the surcharge load q = 10 kPa, the axial load increased from zero at y =1.5 m to 4.09 kN/m at y = 0.75 m (just above the reinforcement). The down-drag load (0.66 kN/m) from the steel strips resulted in a jump in facing axial load from 4.09 to 4.75 kN/m at y = 0.75 m. The reinforcement connection segment in **Figure 2c** has a slope of 0.005 m/0.05 m = 1/10. Thus, based on the reinforcement connection load of 6.52 kN/m at q = 10 kPa the down-drag force from the reinforcement is 6.52×sin($\tan^{-1}$(1/10)) = 0.65 kN/m. This confirms that the sharp change in facing axial load is from the down-drag load in the reinforcement due to the connection geometry in **Figure 2c**. The facing panel axial load continued increasing to 9.15 kN/m at bottom of the facing (y = 0). For q = 50 kPa, the down-drag load from the reinforcement was about 2.27 kN/m and the maximum facing axial load was about 15.9 kN/m at y = 0. When the surcharge load was increased to q = 100 kPa, the down-drag load from the reinforcement increased to 4.28 kN/m and the maximum facing load increased to 24.3 kN/m. In conclusion, the results from both programs agreed very well when geogrid elements in PLAXIS and beam elements in FLAC were used to model the reinforcement for Case 3.

4.6 Reinforcement Modelled by Structure Elements without Normal Stiffness for Case 3

The use of different structure elements in FLAC resulted in different facing axial loads for Case 2. In this section the effect of different structure elements on the reinforcement tensile loads and facing axial loads for Case 3 are examined. The reinforcement axial loads are shown in **Figure 11** for the reinforcement using strip elements in FLAC. Again very good agreement was observed between the strip elements in FLAC (**Figure 11**) and beam elements in FLAC (**Figure 9**) for reinforcement axial loads. When comparing the predicted reinforcement axial loads from FLAC (with strip elements) with those from PLAXIS (with geogrid elements), the maximum difference was within 2% for q = 100 kPa.

Figure 12 shows the facing axial loads using strip elements in FLAC. Differences in facing axial loads are minor when using beam (**Figure 10**) and strip (**Figure 12**) elements in FLAC. When comparing the predicted facing axial loads from FLAC (with strip elements) with those from PLAXIS (with geogrid elements), the maximum difference was within 10% near y = 0.75 m for the surcharge load q = 100 kPa. The modeling results show that for Case 3, the reinforcement tensile loads and facing axial loads between different structure elements and between different programs agree very well.

4.7 Effect of Backfill Soil Modulus for Case 3

Figure 13 shows the effect of the backfill soil modulus value on the reinforcement axial loads using FLAC and PLAXIS. Compared to the results with E_{soil} = 5 MPa in **Figure 9**, increasing the backfill soil modulus to E_{soil} = 50 MPa (**Figure 13**) decreased the tensile loads in the reinforcement when other conditions remained the same (i.e., interface property values kept the same using the second option described in **Section 2.3**). The slight differences in tensile loads occur for the beam elements in FLAC and geogrid elements in PLAXIS when q = 50 and 100 kPa and are due to the small differences in predicted displacements. Thus the results show that greater backfill modulus and larger surcharge load have more effect on the differences in predicted reinforcement tensile loads between FLAC and PLAXIS than cases with lower values.

Figure 14 shows the facing panel axial loads for the case of backfill soil modulus E_{soil} = 50 MPa. The higher modulus of the backfill soil resulted in lower facing axial loads when compared to those with E_{soil} = 5 MPa in **Figure 10** and is attributed to less soil deformation due to the greater backfill soil modulus. The facing axial loads using FLAC generally agreed well with those from PLAXIS. The slight differences in facing axial loads were because of small differences in down-drag loads predicted using the two programs as shown in **Figure 13**.

4.8 Effect of Interface Stiffness for Case 3

The magnitude of the normal and shear loads transferred from the backfill soil to the reinforcement and facing panel is controlled by the interface stiffness and shear strength. **Figure 15** shows the effect of the interface stiffness on the reinforcement tensile loads. When compared to the tensile loads of the reinforcement with k_n = 49.7 MPa/m and k_s = 4.51 MPa/m in **Figure 9**, the increase in interface stiffness (k_n = 497 MPa/m and k_s = 45.1 MPa/m) increased the reinforcement tensile loads (**Figure 15**). The data in **Figure 15** show that the reinforcement tensile loads using FLAC agree very well with those using PLAXIS even for cases with higher interface stiffness.

The effect of the interface stiffness on the facing axial loads is shown in **Figure 16**. The higher interface stiffness (k_n = 497 MPa/m and k_s = 45.1 MPa/m) in **Figure 16** resulted in larger facing axial loads when compared to results in **Figure 10** with k_n = 49.7 MPa/m and k_s = 4.51 MPa/m. The predicted facing axial loads from FLAC agree well with those from PLAXIS as shown in **Figure 16** for the higher interface stiffness.

4.9 Effect of Contact Area between Soil and Reinforcement for Case 3

The results reported in previous sections for Case 3 are very encouraging because the predictions for facing axial loads, reinforcement axial loads are generally in very good agreement using both programs. However, the out-of-plane width of the steel reinforcement is 0.1 m (less than 0.675 m as noted earlier in the paper and the interface with out-of-plane width of 0.675 m was assumed in the previous sections for Cases 2 and 3). The geogrid elements in PLAXIS and beam elements in FLAC with interfaces between the structure elements and backfill soil assume that the reinforcement is continuous in the out-of-plane direction. However, the cable and strip elements in FLAC can be used to model both continuous and discontinuous structures in the out-of-plane direction. In this section, the out-of-plane width of 0.1 m for the steel strip was modelled using strip elements.

The reinforcement axial loads from FLAC with strip elements are shown in **Figure 17**. The FLAC results clearly show that, when the 0.1-m wide steel strip was modelled, the reinforcement axial loads were lower than those assumed using a 0.675-m wide steel strip in PLAXIS (for the same reinforcement axial stiffness computed, i.e., $E_{steel} \times A_s$). The reduced contact area between the 0.1-m wide steel strip and backfill soil was the main reason for the lower reinforcement axial loads when compared to the assumed 0.675-m wide steel strip in PLAXIS.

Figure 18 shows the facing panel axial loads using strip elements with the out-of-plane width of 0.1 m in FLAC. Predicted facing axial loads using PLAXIS with geogrid elements (out-of-plane width of 0.675 m), were similar to facing axial loads over the range y = 0.75 to 1.5 m but facing axial loads were visibly lower for y = 0 to 0.75 m using FLAC with strip elements (out-of-plane width of 0.1 m). These differences increased with increasing surcharge load. The differences in facing axial loads were due to lower reinforcement loads (**Figure 17**) resulting in less down-drag forces using FLAC with 0.1-m wide steel strip when compared to PLAXIS with assumed 0.675-m wide steel strip.

5 Conclusions

A number of commercially available software programs are available to geotechnical design engineers and researchers to predict the behaviour of reinforced soil walls (MSE walls). Most programs are based on the finite element method. An example program is PLAXIS **(2008)**. Another widely used software program is FLAC (**Itasca 2011**) which is based on the finite difference method. The treatment of soil-facing interfaces and the inclusions used to model the reinforcing layers in MSE walls also vary between and within the programs. Potential quantitative differences in numerical predictions for nominally identical wall cases using these two programs are of interest to both designers and researchers. This is the motivation for the work described in this paper.

Numerical predictions using both programs were focused on reinforced soil–facing panel interaction with equivalent interface properties based on the Mohr-Coulomb failure criterion. The numerical analyses using unit cells showed that for the same surcharge loads and applied lateral displacement for the upper cell the predicted normal and shear stresses and normal displacements from both computer programs agreed very well. A MSE wall model segment with and without steel reinforcement was used to demonstrate how the reinforcement can be modelled in both programs using interfaces with zero thickness to capture soil-structure interactions. Based on the cases and conditions examined, the following conclusions can be made:

- The predicted normal and shear stresses between the facing panel and backfill soil using FLAC generally agreed well with those from PLAXIS (Case 1 shown in **Figure 2a**). The slight differences in normal and shear stresses between the two programs were due to very small differences in predicted plastic displacements.

- Considering the steel reinforcement with out-of-plane width of 0.675 m (Case 2 shown in **Figure 2b**), the tensile loads of the reinforcement agreed well between FLAC (beam, cable, strip elements) and PLAXIS (geogrid elements). However, the facing panel axial loads using FLAC with cable and strip elements were different from those using FLAC with beam elements and PLAXIS with geogrid elements.
- When the steel reinforcement was assumed to be 0.675 m wide (Case 3 shown in **Figure 2c**), both programs predicted similar results for facing and reinforcement axial loads even though the reinforcement was modelled using different structure elements (geogrid in PLAXIS, and beam, cable, and strip in FLAC).
- Increasing the backfill soil modulus decreased both the reinforcement tensile loads and facing axial loads. Small differences in the reinforcement tensile loads and facing axial loads were observed between FLAC and PLAXIS results for larger backfill soil modulus values and larger surcharge loads (other conditions being equal).
- Increasing the interface stiffness increased both the reinforcement tensile loads and facing axial loads. The numerical results from both FLAC and PLAXIS agreed very well.
- Modelling the true out-of-plane width of 0.1 m for the steel strip with cable and strip elements in FLAC resulted in lower reinforcement axial load and less down-drag forces on the facing panel when compared to results from both FLAC and PLAXIS using the assumed out-of-plane width of 0.675 m (using the same reinforcement axial stiffness).
- For the case of soil reinforcement materials which are discontinuous in the out-of-plane direction, program PLAXIS with geogrid elements and program FLAC using beam elements use larger interface area and therefore predict greater reinforcement axial loads than program FLAC using cable and strip elements.

Despite the potential for different quantitative predictions depending on which program is used and which options and constitutive models available in each program are adopted, both programs have been used to reproduce the measured performance of instrumented full-scale walls to acceptable accuracy by adjusting soil parameter values within reasonable limits to improve agreement (e.g., **Hatami et al. 2005, 2006; Huang et al. 2009; Damians et al. 2014a**).

Acknowledgements

The work reported in this paper was supported by grants from the Natural Sciences and Engineering Research Council of Canada (NSERC) awarded to the third author. The second author wishes to acknowledge the support of the Universitat Politècnica de Catalunya (UPC-BarcelonaTech) and the funding received through the research project BIA2010-20789-C04-01 from the Ministry of Education and Innovation of Spain.

References

AASHTO 2012. LRFD Bridge Design Specifications, American Association of State Highway and Transportation Officials (AASHTO), 6th Ed., Washington, DC.

Abdelouhab, A., Dias, D. and Freitag N. 2011. Numerical analysis of the behaviour of mechanically stabilized earth walls reinforced with different types of strips. *Geotextiles and Geomembranes*, 29: 116-129.

Allen, T.M., Bathurst, R.J., Holtz, R.D., Lee, W.F. and Walters, D.L. 2004. A New Working Stress Method for Prediction of Loads in Steel Reinforced Soil Walls, ASCE Journal of Geotechnical and Geoenvironmental Engineering. 130(11): 1109-1120.

BS8006 2010. Code of Practice for Strengthened/Reinforced Soil and Other Fills, British Standards Institution (BSI). Milton Keynes, UK.

Cai, Z. and Bathurst, R.J. 1995. Seismic response analysis of geosynthetic reinforced soil segmental retaining walls by finite element method. *Computers and Geotechnics*, 17(4): 523-546.

Damians, I.P., Bathurst, R.J., Josa, A., Lloret, A. and Albuquerque, P.J.R. 2013. Vertical facing loads in steel reinforced soil walls. *Journal of Geotechnical and Geoenvironmental Engineering* (ASCE), 139(9): 1419-1432.

Damians, I.P., Bathurst, R.J., Josa, A. and Lloret, A. 2014a. Numerical analysis of an instrumented steel reinforced soil wall. *International Journal of Geomechanics* (ASCE), (online)

Damians, I.P., Bathurst, R.J., Josa, A. and Lloret, A. 2014b. Numerical study of the influence of foundation compressibility and reinforcement stiffness on the behavior of reinforced soil walls. *International Journal of Geotechnical Engineering*, 8(3): 247-259.

Hatami, K. and Bathurst, R.J. 2005. Development and verification of a numerical model for the analysis of geosynthetic reinforced soil segmental walls under working stress conditions. *Canadian Geotechnical Journal*, 42(4): 1066-1085.

Hatami, K. and Bathurst, R.J. 2006. Numerical model for reinforced soil segmental walls under surcharge loading. *Journal of Geotechnical and Geoenvironmental Engineering* (ASCE), 132(6): 673-684.

Hatami, K., Bathurst, R.J. and Di Pietro, P. 2001. Static response of reinforced soil retaining walls with non-uniform reinforcement. *International Journal of Geomechanics*, 1(4), 477-506, 2001

Huang, B., Bathurst, R.J. and Hatami, K. 2009. Numerical study of reinforced soil segmental walls using three different constitutive soil models. *Journal of Geotechnical and Geoenvironmental Engineering* (ASCE), 135(10): 1486-1498.

Huang, B., Bathurst, R.J., Hatami, K. and Allen, T.M. 2010. Influence of toe restraint on reinforced soil segmental walls. *Canadian Geotechnical Journal*, 47(8): 885-904.

Itasca. 2011. FLAC: Fast Lagrangian Analysis of Continua. Version 7.0 [computer program]. Itasca Consulting Group, Inc., Minneapolis, Minn.

Karpurapu, R.G. and Bathurst, R.J. 1995. Behaviour of geosynthetic reinforced soil retaining walls using the finite element method. *Computers and Geotechnics*, 17(3): 279-299.

Ng, P.C.F., Pyrah, I.C. and Anderson, W.F. 1997. Assessment of three interface elements and modification of the interface element in CRISP90. *Computers and Geotechnics*, 21(4): 315-339.

PLAXIS. 2008. *Reference manual*, 2D - version 9.0, PLAXIS, Delft University of Technology, Delft, Netherlands.

Rowe, R.K. and Ho, S.K. 1997. Continuous panel reinforced soil walls on rigid foundations. *Journal of Geotechnical and Geoenvironmental Engineering*, 123(10), 912-920.

Yoo, C., Jang, Y.S. and Park, I.J. 2011. Internal stability of geosynthetic-reinforced soil walls in tiered configuration. *Geosynthetics International*, 18(2), 74-83.

Table 1. Property values for unit cells (Note: the property values for the soil are unconstrained because all boundaries of the bottom soil cell are fixed in *x*- and *y*-direction)

Parameter	Value	Program[1]
Concrete		
Unit weight, γ_{conc} (kN/m^3)	0	F and P
Young's modulus, E_{conc} (GPa)	32.0	F and P
Poisson's ratio, v_{conc} (-)	0.15	F and P
Interface		
Interface friction angle, φ_i (degree)	40.0	F and P
Adhesion, c_i (kPa)	1.0	F and P
Dilation angle, ψ_i (degree)	0	F and P
Tension strength, $\sigma_{t,i}$ (kPa)	0	F and P
Young's modulus, E_i (MPa)	0.82	P
Poisson's ratio, v_i (-)	0.45	P
Compression modulus, $E_{oed,i}$ (MPa)	3.11	P
Shear modulus, G_i (MPa)	0.283	P
Virtual interface thickness, t_i (m)	0.283	P
Normal stiffness, k_n (MPa/m)	11.0	F
Shear stiffness, k_s (MPa/m)	1.0	F

Note: [1] F and P denote FLAC and PLAXIS computer programs, respectively;

Table 2. Property values for model with single precast concrete panel segment and single layer of soil reinforcement

Parameter	Value	Program[1]
Concrete panel		
Unit weight, γ_{conc} (kN/m^3)	24.0	F and P
Young's modulus, E_{conc} (GPa)	32.0	F and P
Poisson's ratio, v_{conc} (-)	0.15	P
Cross-sectional area[2], A_p (m^2)	0.18	F
Moment of inertia[2], I_p (m^4)	4.86×10^{-4}	F
Axial stiffness[2], $E_{conc}A_p$ (GN/m)	5.76	P
Bending stiffness[2], $E_{conc}I_p$ (MN/m^2/m)	15.6	P
Backfill soil		
Unit weight, γ_{soil} (kN/m^3)	18.0	F and P
Friction angle, φ_{soil} (degree)	44.0	F and P
Cohesion, c_{soil} (kPa)	1.0	F and P
Dilation angle, ψ_{soil} (degree)	14.0	F and P
Tension strength, $\sigma_{t,soil}$ (kPa)	0	F and P
Young's modulus, E_{soil} (MPa)	5.0	F and P
Poisson's ratio, v_{soil} (-)	0.3	F and P
Steel reinforcement		
Young's modulus, E_{steel} (GPa)	200	F
Scaled cross-sectional area[3], A_s (m^2/m)	3.41×10^{-4}	F
Moment of inertia, I_p (m^4)	0	F
Scaled axial stiffness[3], $E_{steel}A_s$ (MN/m)	68.2	P
Interface		
Friction angle, φ_i (degree)	16.2	F and P
Cohesion, c_i (kPa)	0.3	F and P
Dilation angle, ψ_i (degree)	0	F and P
Tension strength, $\sigma_{t,i}$ (kPa)	0	F and P
Young's modulus, E_i (MPa)	0.502	P
Poisson's ratio, v_i (-)	0.45	P
Compression modulus, $E_{oed,i}$ (MPa)	1.90	P
Shear modulus, G_i (MPa)	0.173	P
Virtual interface thickness, t_i (m)	0.0383	P
Normal stiffness, k_n (MPa/m)	49.7	F
Shear stiffness, k_s (MPa/m)	4.51	F

Note: [1] F and P denote FLAC and PLAXIS computer programs, respectively; [2] based on out-of-plane width of 1 m and the unit of the variable based on corresponding computer program manual; [3] the value is scaled to 1.0 m out-of-plane width for plane strain calculation.

Table 3. Cable and strip property values in FLAC

Parameter[1]	Value
Cable element	
Exposed perimeter, *perimeter* (m)	0.2 (1.3)
Cross-sectional area, *area* (m^2)	2.3×10^{-4}
Grout stiffness[2], *kbond* (MN/m/m)	0.903 (6.09)
Grout cohesion[3], *sbond* (kN/m)	0.06 (0.405)
Grout frictional resistance, *sfriction* (degree)	16.2
Spacing, *spacing* (m)	0.675
Out-of-plane stress component, s_{zz} (-)	off
Strip element	
Calculation width, *calwidth* (m)	0.675
Number of strips per calculation width, *nstrips* (-)	1
Initial apparent friction coefficient, *fstar0* (-)	0.3
Minimum apparent friction coefficient, *fstar1* (-)	0.3
Strip/interface shear stiffness[4], *strkbond* (MN/m/m)	0.903 (6.09)
Strip/interface cohesion[5], *strsbond* (kN/m)	0.06 (0.405)
Strip width, *strwidth* (m)	0.1 (0.675)
Strip thickness[6], *strthickness* (m)	2.3×10^{-3} (3.41×10^{-4})

Note: [1] italicized parameter names are used in the FLAC manual.
[2] *kbond* = k_s×*perimeter*;
[3] *sbond* = c_i×*perimeter*;
[4] *strkbond* = k_s×2×*strwidth*;
[5] *strsbond* = c_i×2×*strwidth*;
[6] to keep the same cross-sectional area of 2.3×10^{-4} m^2 (*strwidth*×*strthickness*) and therefore the same axial stiffness.

Table 4. Numerical results for the soil-concrete interface response between unit cells

Applied surcharge load (kPa)	Applied displacement (mm)	Soil-concrete interface ($k_n = 1.1 \times 10^7$ Pa/m, $k_s = 1.0 \times 10^6$ Pa/m)						
		Normal displacement (mm)			Shear stress (kPa)			Shear stress state
		FLAC	PLAXIS	Analytical	FLAC	PLAXIS	Analytical	
q = 10	5	0.909	0.910	0.909	5.00	5.00	5.00	Elastic
	10				9.39	9.40	9.39	Plastic
	15				9.39	9.40	9.39	Plastic
	20				9.39	9.40	9.39	Plastic
q = 50	20	4.55	4.55	4.55	20.0	20.0	20.0	Elastic
	40				40.0	40.0	40.0	Elastic
	60				43.0	43.0	43.0	Plastic
	80				43.0	43.0	43.0	Plastic
q = 100	80	9.09	9.10	9.09	80.0	80.0	80.0	Elastic
	100				84.9	85.0	84.9	Plastic
	120				84.9	85.0	84.9	Plastic
	140				84.9	85.0	84.9	Plastic

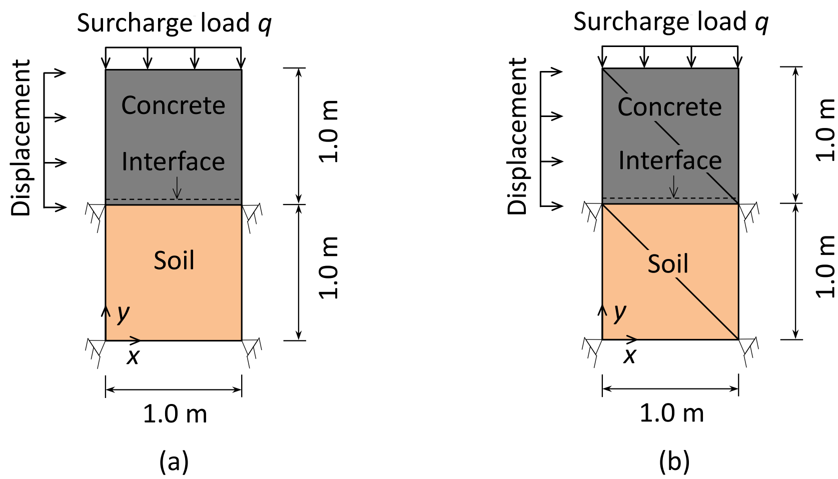

Figure 1. Schematic showing unit cells with concrete-soil interface: (a) boundary conditions and finite difference numerical grid with FLAC and (b) boundary conditions and finite element mesh with PLAXIS (Note: for boundary conditions and concrete material modulus examined, the number of zones in FLAC and elements in PLAXIS does not affect numerical results)

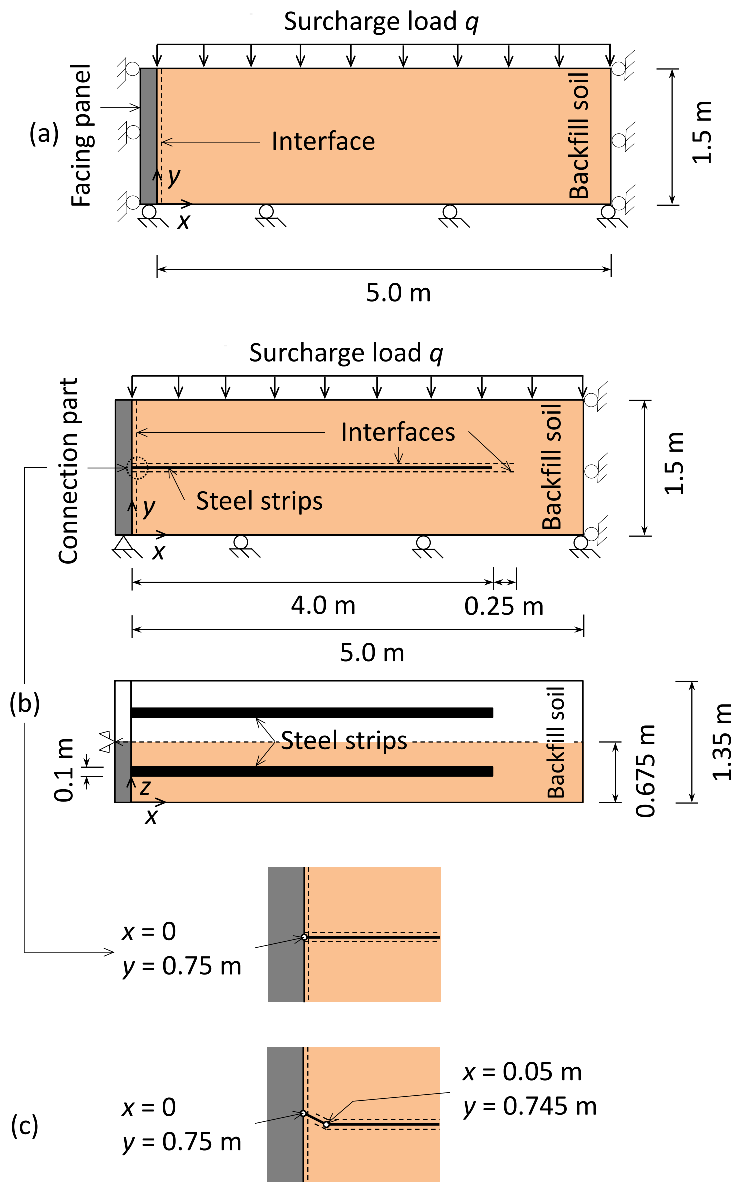

Figure 2. Schematic showing single precast concrete panel wall segment: (a) without steel strips, (b) with steel strips defined horizontally, and (c) with steel strips defined specially at the connection part (Note: the extension of interfaces between the steel strips and backfill is applied only when using PLAXIS; *x* is the horizontal direction; *y* is the vertical direction; *z* is the out-of-plane direction)

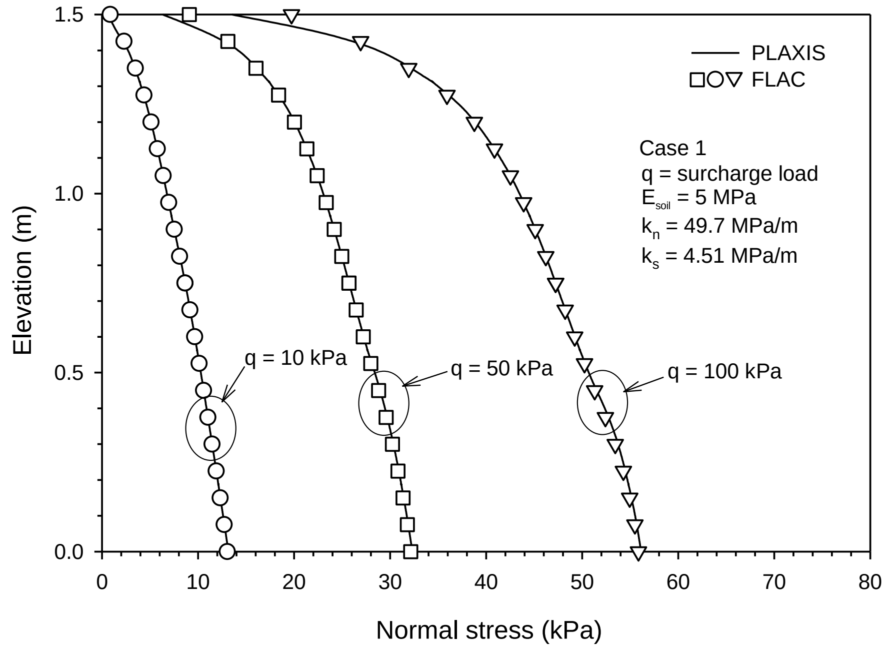

(a)

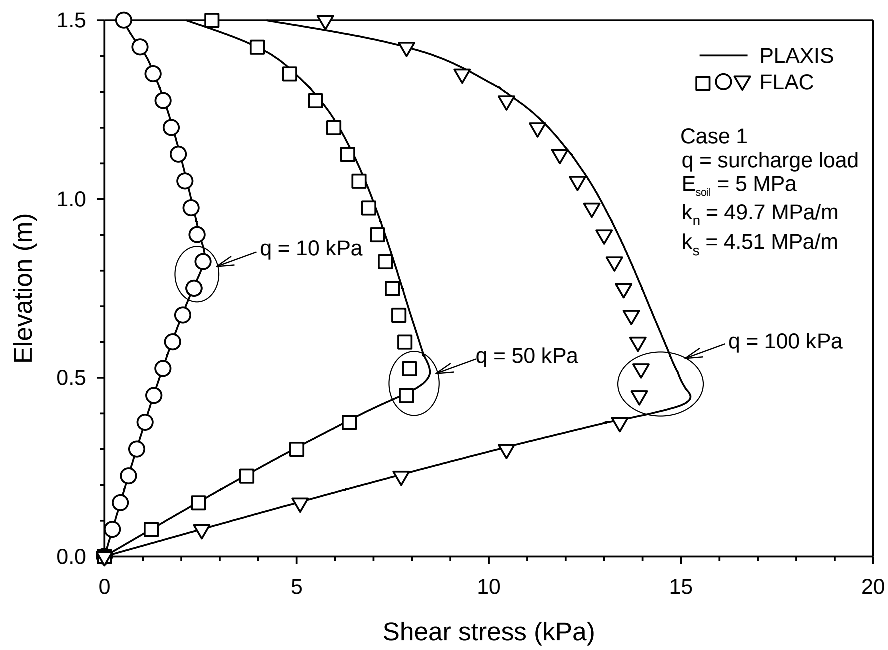

(b)

Figure 3. Load transfer from backfill soil to facing panel (Case 1): (a) normal stress and (b) shear stress

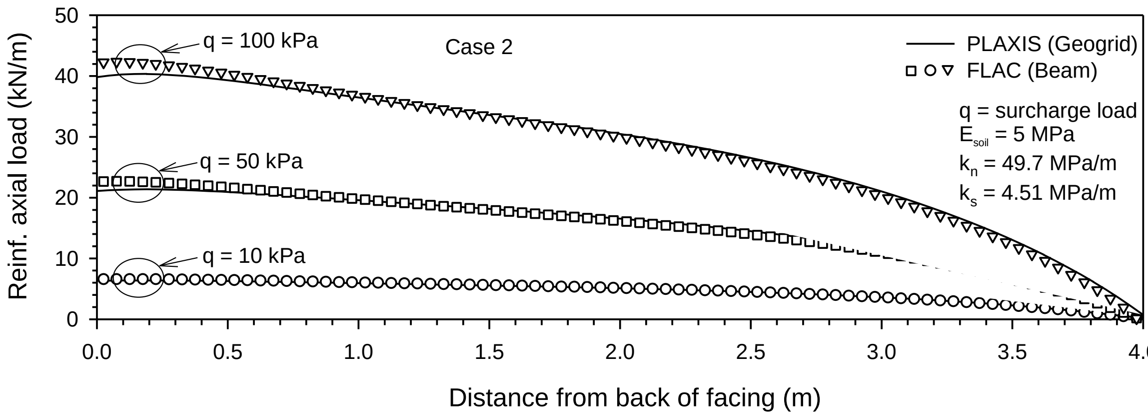

Figure 4. Reinforcement axial loads (Case 2) using PLAXIS geogrid elements and FLAC beam elements

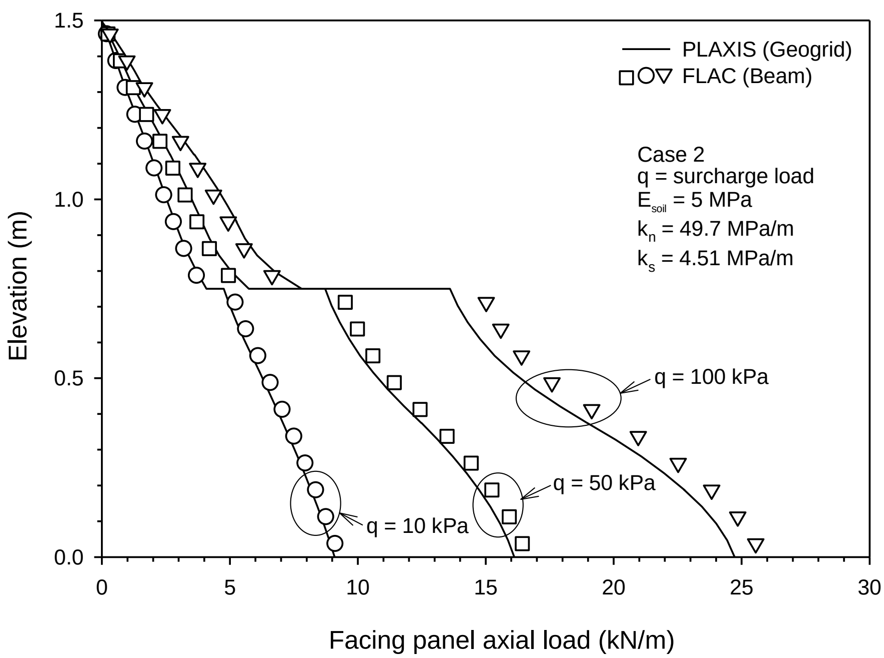

Figure 5. Facing panel axial loads (Case 2) using PLAXIS geogrid elements and FLAC beam elements

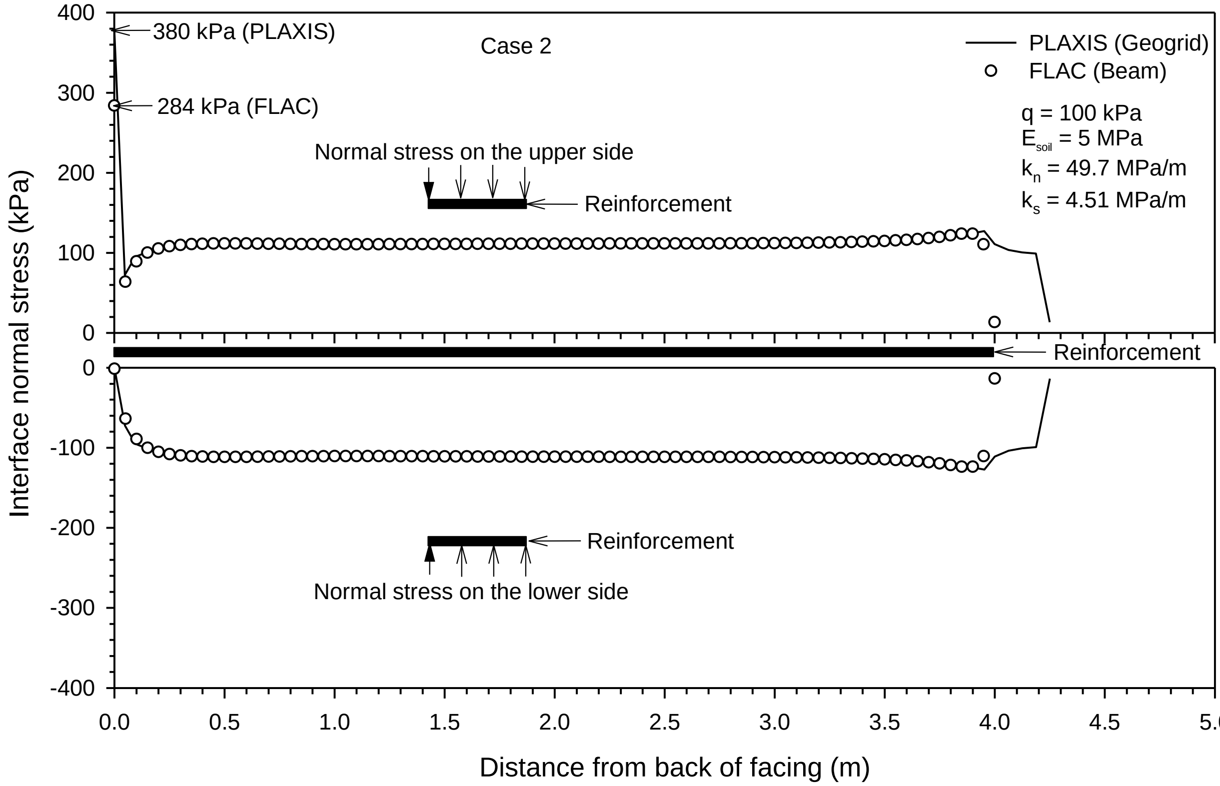

Figure 6. Interface normal stresses on the upper and lower sides of the reinforcement using PLAXIS geogrid elements and FLAC beam elements

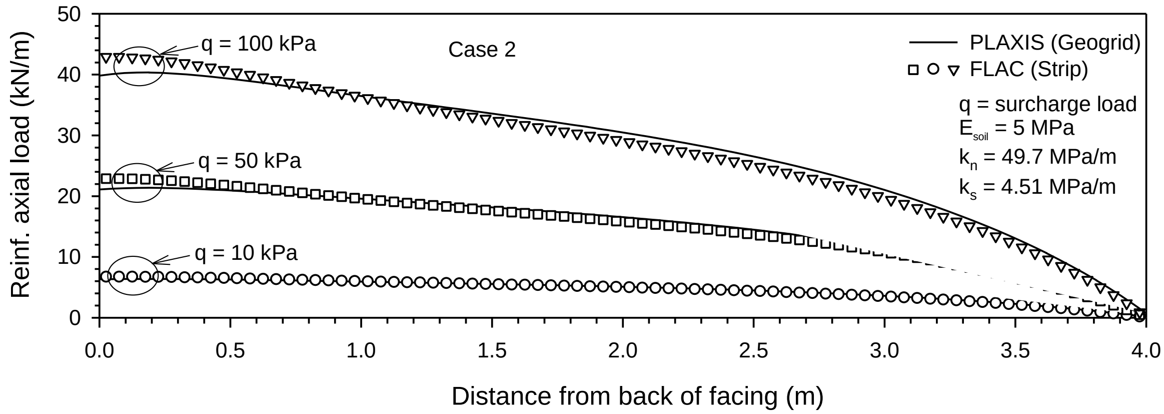

Figure 7. Reinforcement axial loads (Case 2) using PLAXIS geogrid elements and FLAC strip elements

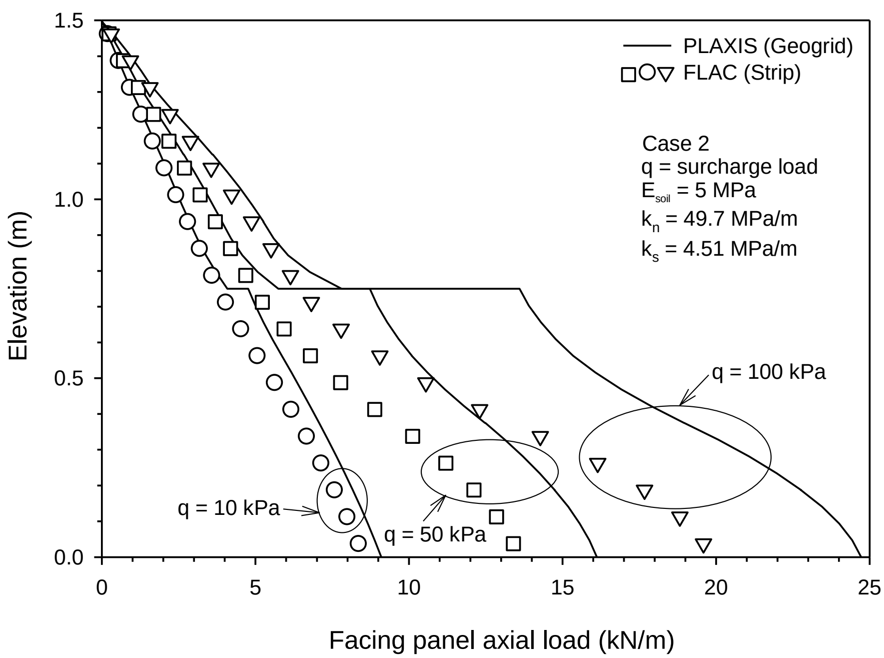

Figure 8. Facing panel axial loads (Case 2) using PLAXIS geogrid elements and FLAC strip elements

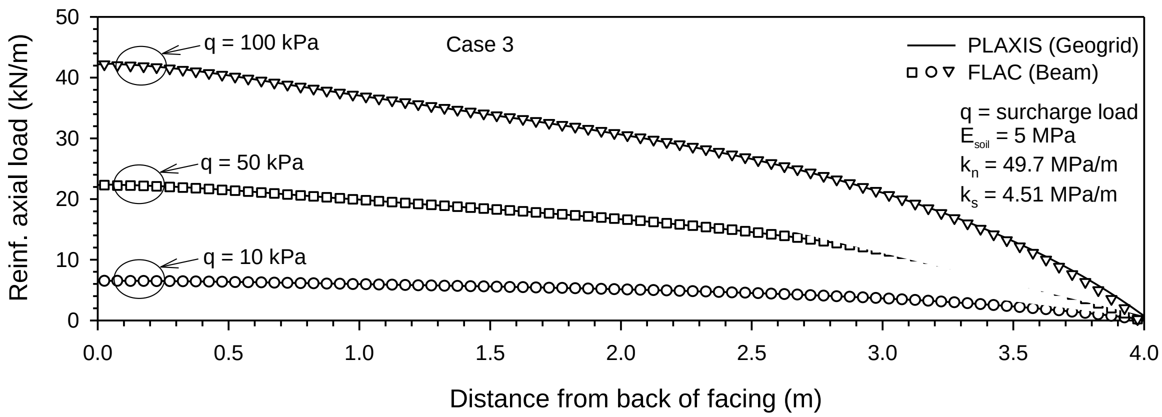

Figure 9. Reinforcement axial loads (Case 3) using PLAXIS geogrid elements and FLAC beam elements

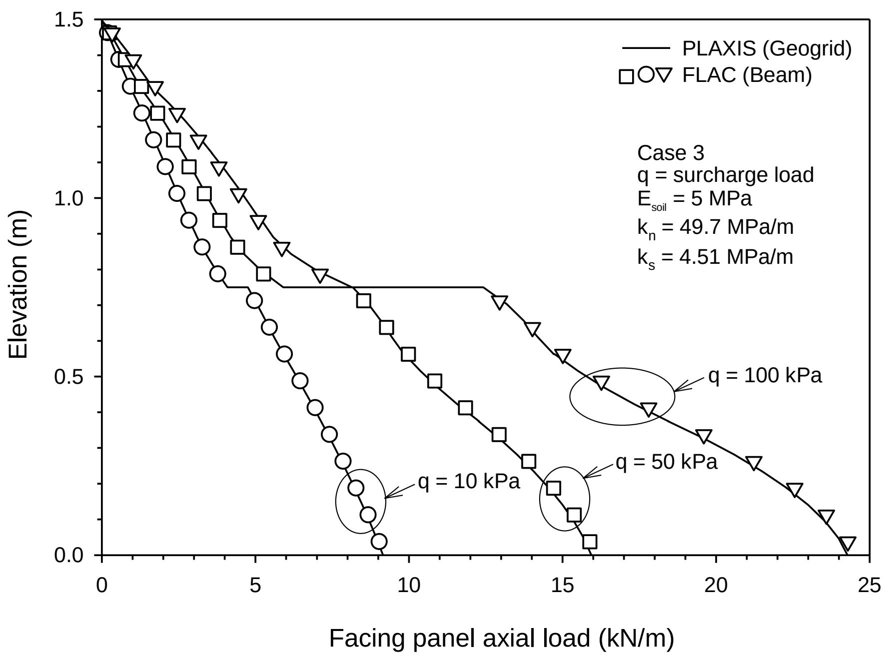

Figure 10. Facing panel axial loads (Case 3) using PLAXIS geogrid elements and FLAC beam elements

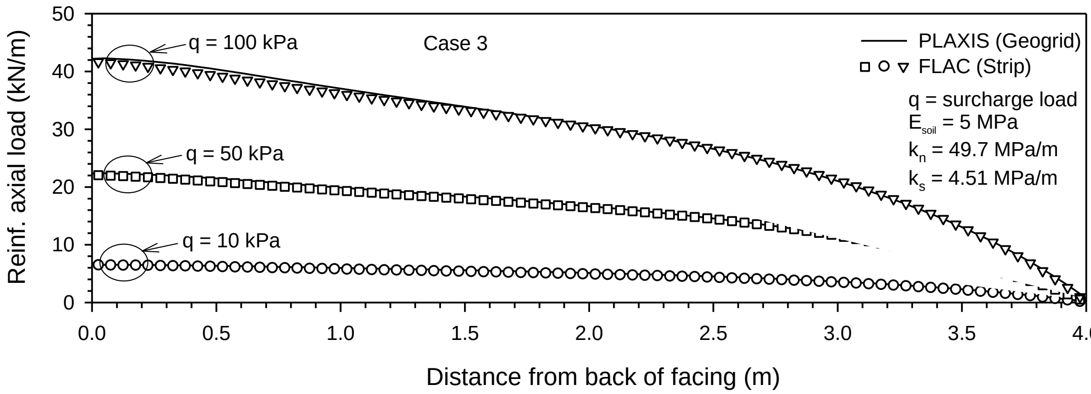

Figure 11. Reinforcement axial loads (Case 3) using PLAXIS geogrid elements and FLAC strip elements

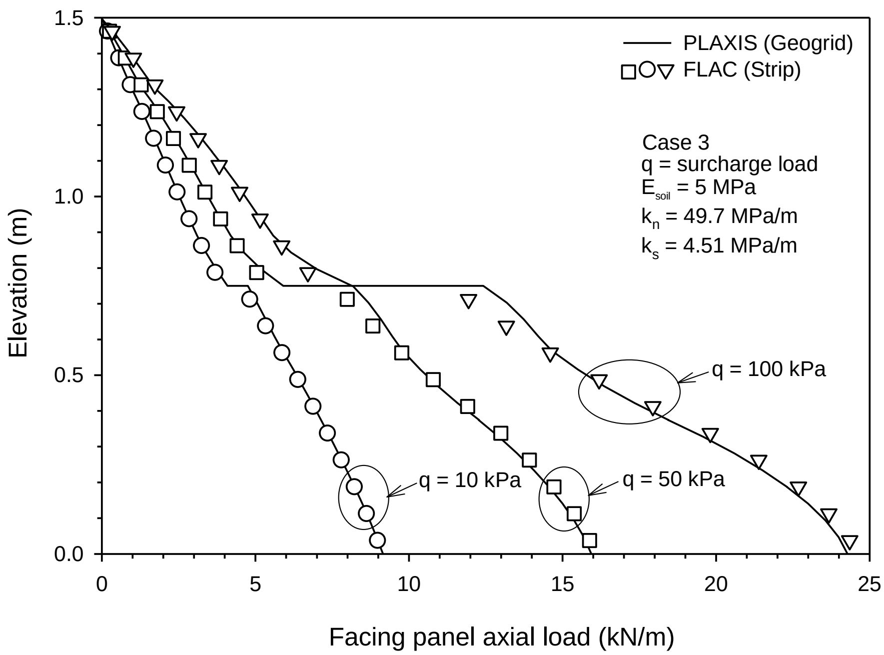

Figure 12. Facing panel axial loads (Case 3) using PLAXIS geogrid elements and FLAC strip elements

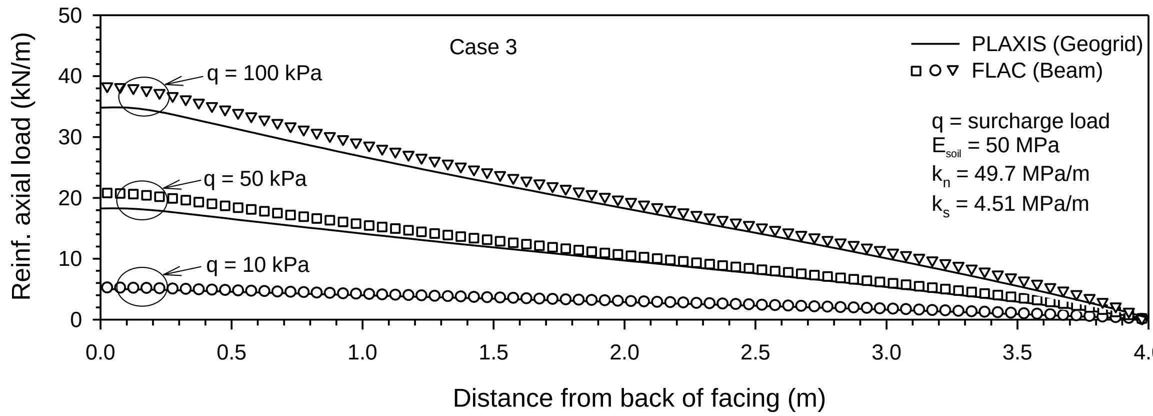

Figure 13. Reinforcement axial loads (Case 3) using PLAXIS geogrid elements and FLAC beam elements with higher Young's modulus of the backfill soil

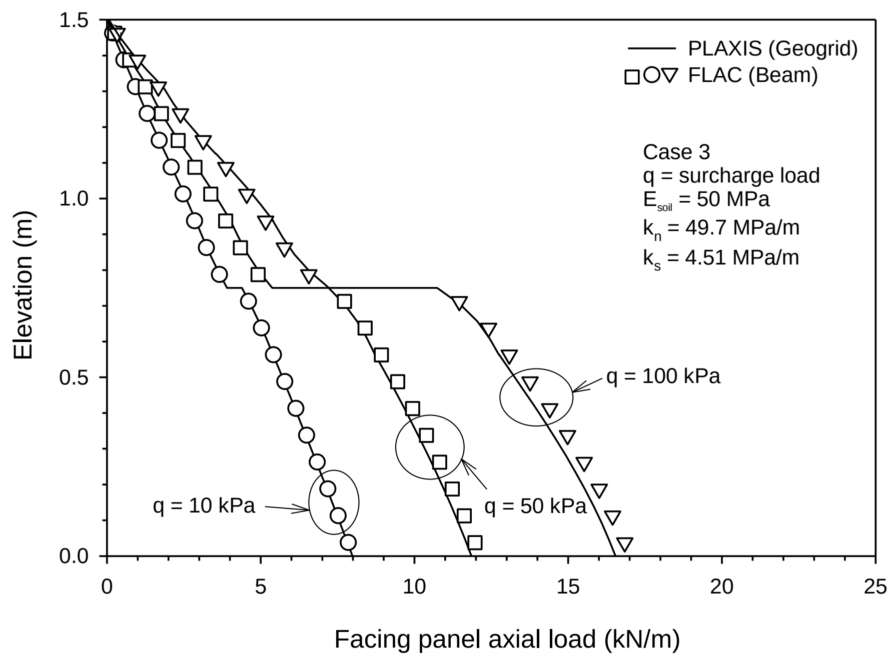

Figure 14. Facing panel axial loads (Case 3) using PLAXIS geogrid elements and FLAC beam elements with higher Young's modulus of the backfill soil

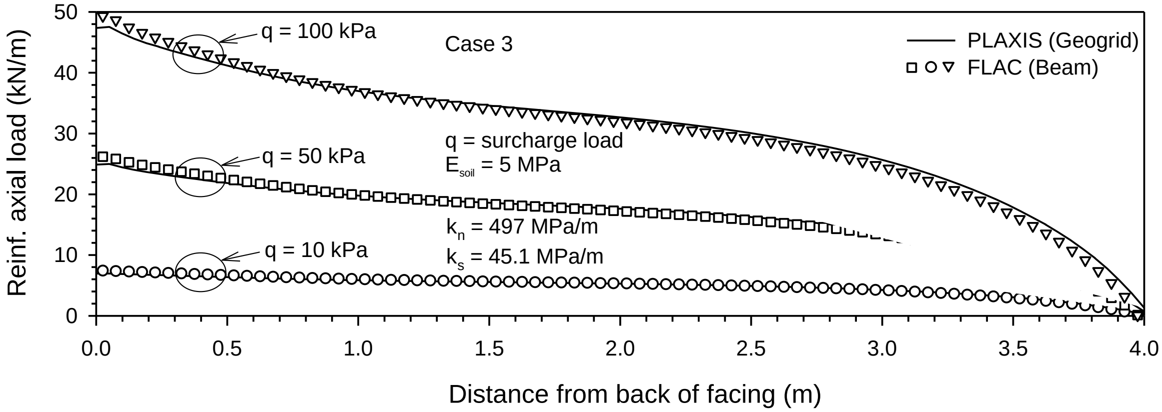

Figure 15. Reinforcement axial loads (Case 3) using PLAXIS geogrid elements and FLAC beam elements with higher interface stiffness

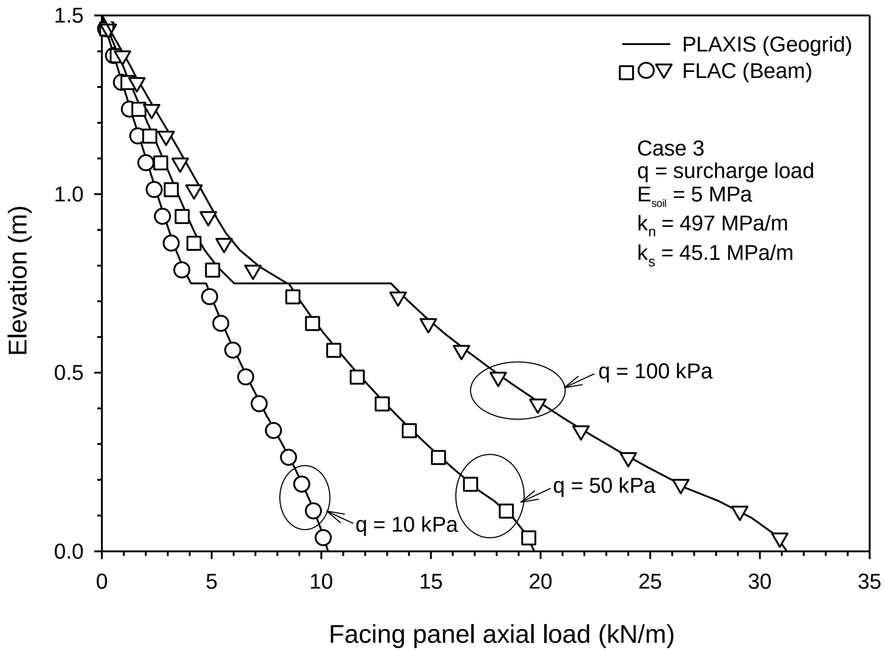

Figure 16. Facing panel axial loads (Case 3) using PLAXIS geogrid elements and FLAC beam elements with higher interface stiffness

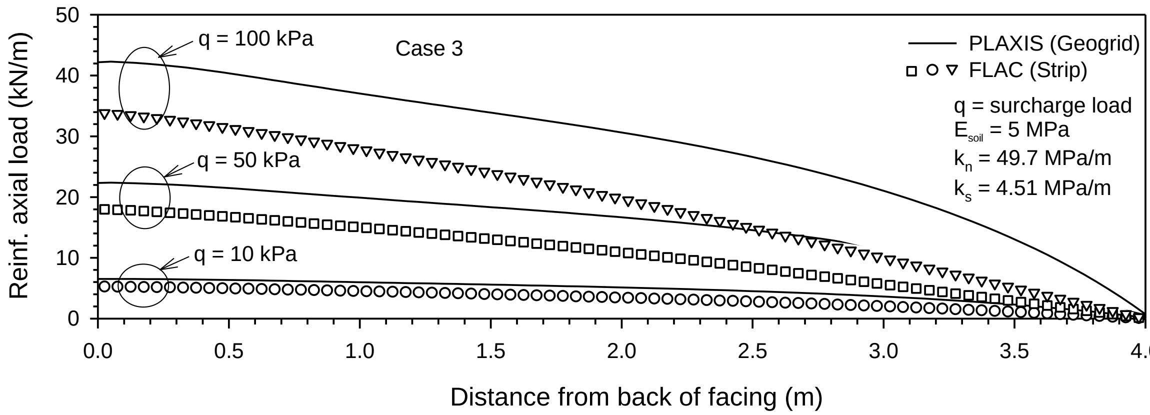

Figure 17. Reinforcement axial loads (Case 3) using PLAXIS geogrid elements (out-of-plane width = 0.675 m) and FLAC strip elements (out-of-plane width = 0.1 m)

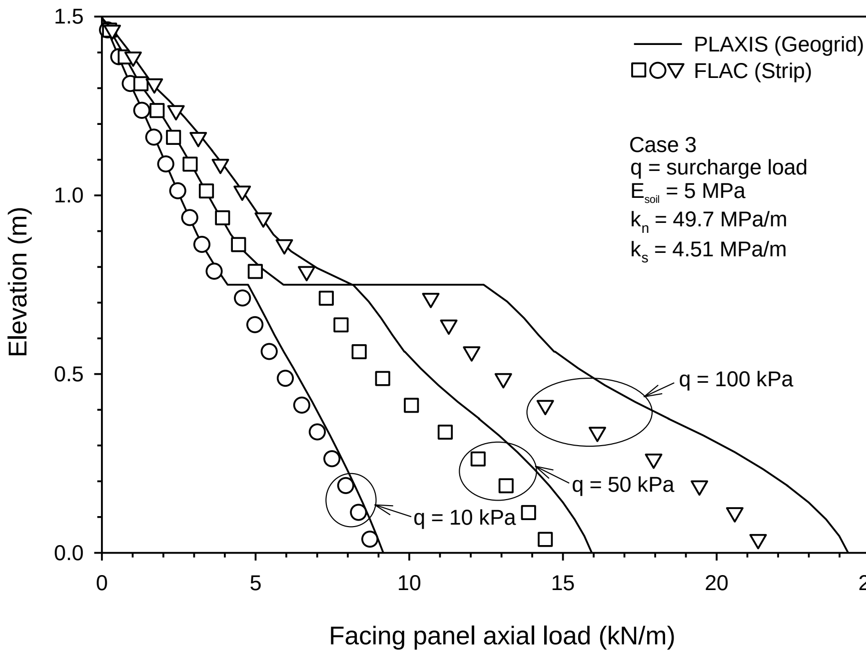

Figure 18. Facing panel axial loads (Case 3) using PLAXIS geogrid (out-of-plane width = 0.675 m) and FLAC strip (out-of-plane width = 0.1 m)